Title	New approach for pole-changing with dual-memory machine
Author(s)	Li, F; Chau, KT; Liu, C; Qiu, C
Citation	IEEE Transactions on Applied Superconductivity, 2014, v. 24 n. 3, article no. 0501504
Issued Date	2014
URL	http://hdl.handle.net/10722/202868
Rights	IEEE Transactions on Applied Superconductivity. Copyright © IEEE.

New Approach for Pole-Changing With Dual-Memory Machine

Fuhua Li, K. T. Chau, *Fellow, IEEE*, Chunhua Liu, *Member, IEEE*, and Chun Qiu

***Abstract*—Memory machines possess the ability of memorizing magnetization level on their permanent magnets (PMs) and hence provide flexible flux-tuning without using the dc field winding for continual excitation. In this paper, two kinds of memory machines, namely the dual-memory and single-memory, are investigated for pole-changing operation with emphasis on the new pole-changing approach for the dual-memory machine. In essence, the dual-memory machine realizes the pole-changing by dropping some poles whereas the single-memory one achieves the pole-changing by reversing some poles. The finite element analysis validates the proposed pole-changing approaches.**

***Index Terms*—Dual-memory, flux-mnemonic machine, memory machine, permanent magnets (PMs) machine, pole-changing.**

I. Introduction

POLE-CHANGING is developed for ac machines offering wide speed range of operation which is particularly desirable for electric vehicles (EVs) [1], [2]. Because of the flexible flux control capability, the memory machines can readily realize the pole-changing [3], [4]. Basically, these memory machines can be divided into two main groups: ac-excited [5], [6] and dc-excited [7], [8]. The ac-excited memory machines employ the d-q axis transformation to derive an armature field component for magnetizing or demagnetizing the permanent magnets (PMs) located in the rotor. The dc-excited memory machines utilize a magnetizing winding to directly magnetize or demagnetize the rotor PMs.

The dc-excited memory machines take the definite advantages of effective online flux control without compromising the torque control. Among them, the single-memory machine utilizes the aluminum-nickel-cobalt (Al-Ni-Co) PM only [9] whereas the dual-memory machine employs both the neodymium-iron-boron (Nd-Fe-B) PM and Al-Ni-Co PM [10]. Actually, the dual-memory machine is derived from the single-memory one, namely the use of Nd-Fe-B PM to improve the overall power density and stability. Because of the high coercivity of Nd-Fe-B PM, the dual-memory and single-memory machines utilize different approaches to achieving the pole-changing.

In this paper, a new pole-changing approach for the dual-memory machine is proposed, and then compared with that of the single-memory machine. Their characteristics and performances at the six-pole and two-pole modes will be analyzed by using the finite element method, and then discussed to verify the validity of the proposed pole-changing approach.

Manuscript received July 16, 2013; accepted November 12, 2013. Date of current version November 22, 2013. This work was supported and funded by a Research Grant (Project No. HKU 710710E) from the Research Grants Council, Hong Kong Special Administrative Region, China.

The authors are with the Department of Electrical and Electronic Engineering, University of Hong Kong, Hong Kong (e-mail: ktchau@eee.hku.hk).

Color versions of one or more of the figures in this paper are available online at http://ieeexplore.ieee.org.

Digital Object Identifier 10.1109/TASC.2013.2291296

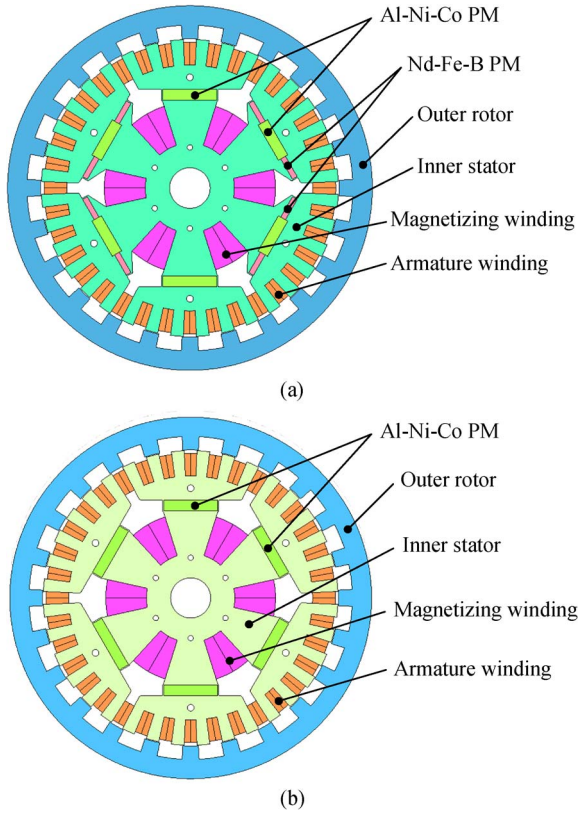

Fig. 1. DC-excited memory machine structures. (a) Dual-memory machine. (b) Single-memory machine.

II. Machine Structure

Fig. 1 shows the machine structures of two dc-excited memory machines. They adopt the outer-rotor arrangement which is particularly suitable for direct-drive in EVs. There are 24 salient poles in the rotor and 30 salient poles in the stator. For the dual-memory machine shown in Fig. 1(a), apart from the two Al-Ni-Co PM poles, there are four PM poles constituted by eight Nd-Fe-B PM pieces and four Al-Ni-Co PM pieces (so-called the 3-magnet PM pole) which are used to perform pole-dropping. Meanwhile, for the single-memory machine shown in Fig. 1(b), each PM pole is based on one piece of Al-Ni-Co PM. Both of them adopt the magnetizing winding to online magnetize or demagnetize the Al-Ni-Co PMs using a positive or negative current pulse, respectively.

TABLE I
MAIN DESIGN PARAMETERS

	Dual-memory	Single-memory
Rated average torque (Nm)	15	12
Diameter (mm)	270	270
Air-gap length (mm)	0.6	0.6
Armature winding (turns)	480	480
Magnetizing winding (turns)	200	200
Weight (kg)	34.7	34.2
PM material	Nd-Fe-B (35AH), Al-Ni-Co (5DG)	Al-Ni-Co (5DG)
Cost (USD)	131	115

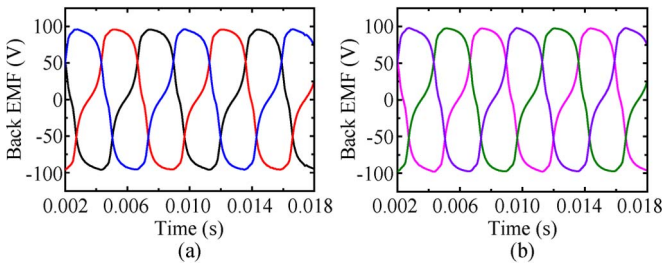

Fig. 2. Back EMF waveforms at six-pole mode. (a) Dual-memory machine. (b) Single-memory machine.

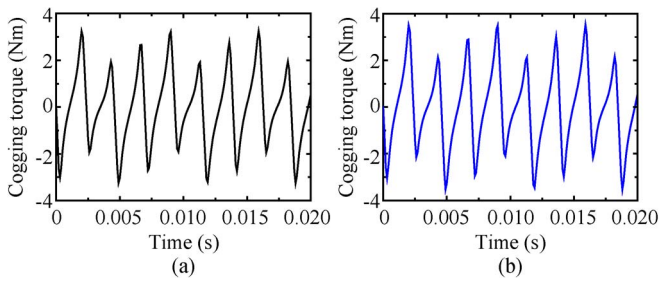

Fig. 3. Cogging torque waveforms at six-pole mode. (a) Dual-memory machine. (b) Single-memory machine.

III. POLE-CHANGING APPROACH

The pole-changing approaches of the two memory machines are simulated by using the finite element software JMAG. The main design parameters are listed in Table I. Also, the sizes of Nd-Fe-B and Al-Ni-Co PMs are selected in such a way that the air-gap flux densities of the two memory machines are comparable.

First, the two memory machines operate at the six-pole mode. When they are driven at 360 rpm, the electromotive force (EMF) waveforms are shown in Fig. 2. Because of similar air-gap flux densities, their EMF amplitudes are also similar. Their trapezoidal EMF shapes facilitate them to operate at the brushless dc mode.

The cogging torque waveforms of the two machines are shown in Fig. 3. They are very similar in both shape and amplitude. It is due to the fact that the cogging torque is mainly governed by remanent flux density of the PM, and both the Al-Ni-Co and Nd-Fe-B PM materials adopted for simulation are of similar remanent flux densities. Meanwhile, Fig. 4 depicts the PM flux in each coil when the armature current is zero. As expected, due to similar air-gap flux densities, the dual-memory and single-memory machines have similar coil flux waveforms in both shapes and amplitudes.

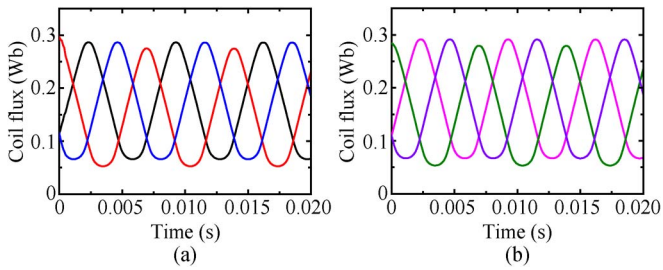

Fig. 4. Coil flux waveforms at six-pole mode. (a) Dual-memory machine. (b) Single-memory machine.

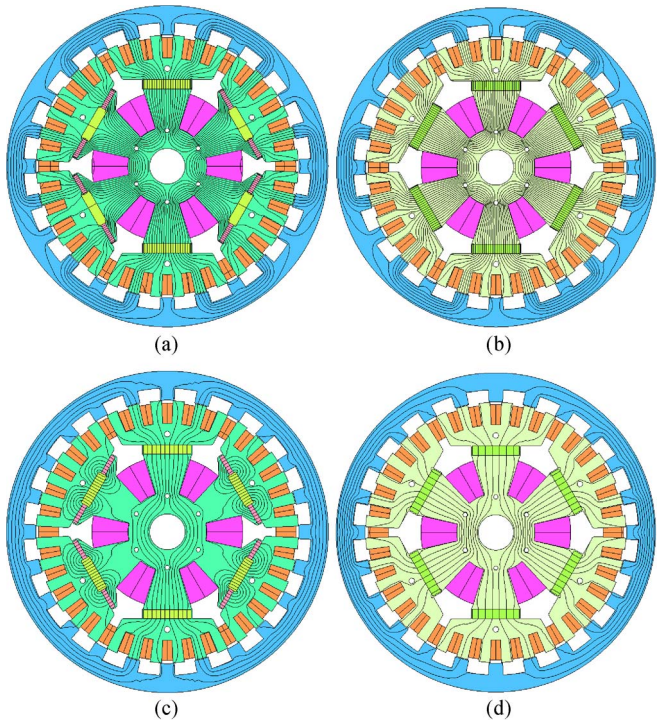

Fig. 5. Flux distributions. (a) Six-pole dual-memory machine. (b) Six-pole single-memory machine. (c) Two-pole dual-memory machine. (d) Two-pole single-memory machine.

Fig. 5 reveals the flux distributions of the two memory machines. Under the six-pole mode, the PM poles are linked uniformly with the neighboring PM poles as shown in Fig. 5(a) and (b) at which the machines have their highest torque capabilities. By applying a negative current pulse in the magnetizing winding to reversely magnetize the Al-Ni-Co PM pieces of the four 3-magnet PM poles, the corresponding Nd-Fe-B PM pieces are magnetically short-circuited as depicted in Fig. 5(c). Namely, all four 3-magnet PM poles are virtually dropped, and the flux lines internally loop within the pole pieces with little contribution to the air-gap field. Thus, the remaining two Al-Ni-Co PM poles serve to provide the desired air-gap flux density. As this pole-dropping can be considered as a specific kind of flux-weakening, there is no need to reconfigure the armature winding. Differing from the dual-memory one, the single-memory machine can magnetize the upper three Al-Ni-Co PM poles to the same polarity and the lower three Al-Ni-Co PM poles to the opposite polarity by applying proper current pulses in the corresponding magnetizing windings. Fig. 5(d) displays the

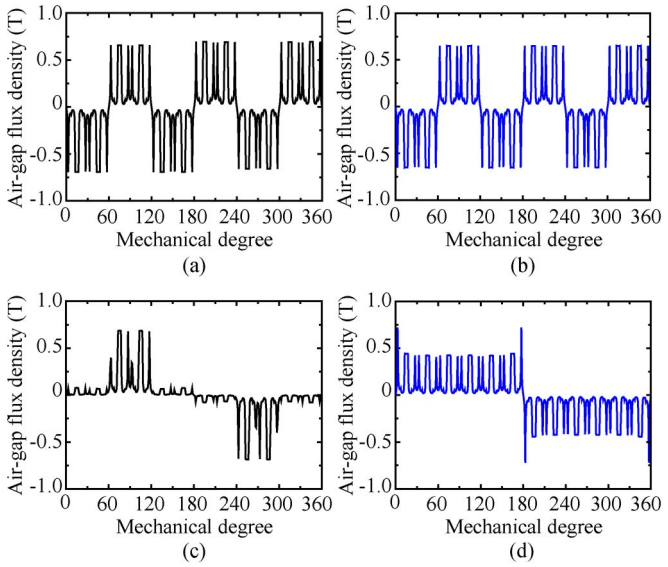

Fig. 6. Air-gap flux density waveforms. (a) Six-pole dual-memory machine. (b) Six-pole single-memory machine. (c) Two-pole dual-memory machine. (d) Two-pole single-memory machine.

flux distribution of the single-memory machine under the two-pole mode. It can be observed that it achieves the pole-changing without dropping any poles. However, the armature winding needs to be reconfigured to enable the two-pole operation.

Focusing on the two-pole mode, the dual-memory machine has only two PM poles contributing flux to the air-gap whereas the single-memory machine has all its six PM poles making such contribution. Thus, the single-memory machine can offer higher air-gap flux and hence higher torque than the dual-memory machine when they are under the two-pole mode.

The air-gap flux density waveforms of the two memory machines under the six-pole and two-pole modes are illustrated in Fig. 6. It is expected that they have similar flux density waveforms under the six-pole pole. However, it can be observed that the air-gap flux density waveform of the dual-memory machine under the two-pole mode clusters at the central regions of two poles whereas the waveform of the single-memory machine spreads over the two poles. Hence, it verifies that the single-memory machine can offer higher air-gap flux than the dual-memory machine under the two-pole mode. Meanwhile, it can be found that the two-pole single-memory machine has lower amplitude of air-gap flux density than the six-pole single-memory one, which is actually due to the magnetic saturation in the rotor iron yoke.

In order to assess the capability of the dual-memory and single-memory machines for wide-range speed control using the proposed pole-changing approaches they are controlled to operate as a PM brushless dc motor [1]. During normal working condition, the machines are fed by a dc-link voltage of 150 V which is higher than the amplitude of back EMF. Fig. 7 shows the output torque waveforms (solid line: instantaneous; dotted line: average) of the two memory machines under the two-pole mode when the armature current is limited to 2 A. It confirms that the average torque of the two-pole dual-memory machine is 2.3 Nm which is only about 39% of the 5.9 Nm of the two-pole single memory machine.

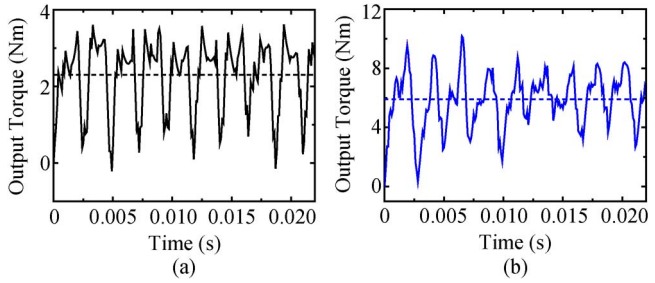

Fig. 7. Output torque waveforms at two-pole mode under normal voltage. (a) Dual-memory machine. (b) Single-memory machine.

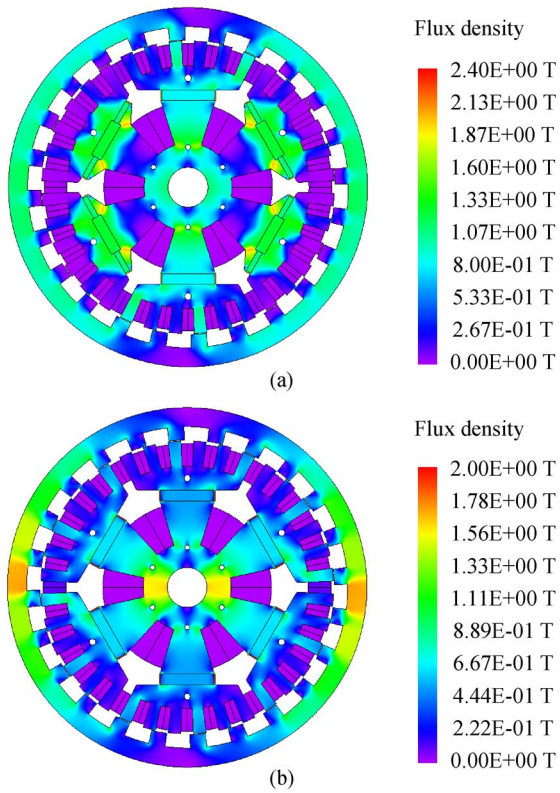

Fig. 8. Flux density distributions at two-pole mode. (a) Dual-memory machine. (b) Single-memory machine.

Fig. 8 presents the flux density distributions of the two memory machines under the two-pole mode. It can be visualized in Fig. 8(a) that the dual-memory machine operates with the two Al-Ni-Co PM poles while dropping the four 3-magnet PM poles. In contrast, as visualized in Fig. 8(b), the single-memory machine operates with six Al-Ni-Co PM poles in which four Al-Ni-Co PMs are reversely magnetized as compared with that for the six-pole mode. Also, it should be observed that there are two regions (the horizontal parts) in the iron yoke of the outer rotor exhibiting high flux densities, which are due to the magnetic saturation. Namely, the thickness of the rotor iron yoke is mainly designed for the normal six-pole mode of operation which needs to fulfill other design criteria such as the moment of inertia and starting torque. If this single-memory machine operates at the two-pole mode under this saturated condition for a long period, the machine efficiency will be degraded.

During the critical working condition, the machines are fed by a dc-link voltage of 100 V which is approximately

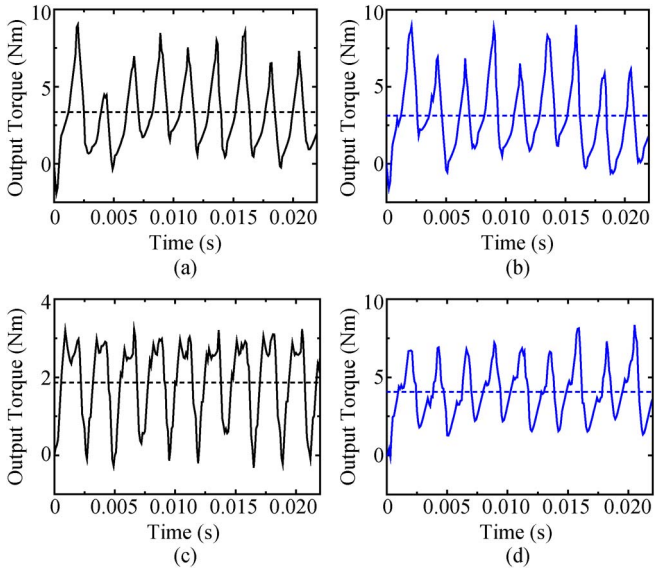

Fig. 9. Output torque waveforms under critical voltage. (a) Six-pole dual-memory machine. (b) Six-pole single-memory machine. (c) Two-pole dual-memory machine. (d) Two-pole single-memory machine.

equal to the amplitude of back EMF. Fig. 9 shows the output torque waveforms (solid line: instantaneous; dotted line: average) of the two memory machines under the six-pole and two-pole modes. It can be observed that the dual-memory machine has an average torque of 3.4 Nm and the single-memory machine has 3.1 Nm under the six-pole mode, indicating that they have similar torque capabilities. It should be noted these two machines are working at the critical speed at which the normal operation can rarely reach, and this speed generally depends on the back EMF and the applied dc-link voltage.

After applying a proper current pulse to the magnetizing winding, the six-pole dual-memory machine becomes a two-pole one and its output torque is reduced to 1.9 Nm (which is about 56% of the torque at the six-pole mode) as shown in Fig. 9(c). It reveals the phenomenon that after dropping the four 3-magnet PM poles, which provide about 2/3 magnetic field, the output torque is reduced by about 44%. This result cannot be achieved at normal working condition. And with this pole-changing capability, the dual-memory machine can work at a higher speed than the critical speed though the output torque also drops in such a way that the output power is maintained less than the rated power.

On the other hand, as shown in Fig. 9(d), the six-pole single-memory machine is changed to the two-pole one and the output torque rises by about 32%, namely from 3.1 Nm to 4.1 Nm. Although both the six-pole and two-pole modes utilize all six Al-Ni-Co PMs, the output torques are different, which is actually due to the effect of magnetic saturation. Namely, in the presence of magnetic saturation, the air-gap flux density decreases; hence, under the critical working condition, as the back EMF decreases, the armature current increases and the output torque also increases.

Therefore, by comparing the performances between the dual-memory and single-memory machines, the dual-memory machine takes the advantages of higher power density and better stability due to the use of Nd-Fe-B PMs, and easier pole-changing due to the use pole-dropping. Particularly, there is no need for this machine to reconfigure the armature winding when performing the pole-dropping. However, the dual-memory machine suffers from lower output torque when operating at the two-pole mode.

It should be noted that the output torque ripples of these memory machines are much higher than traditional PM synchronous machines. Actually, these levels of torque ripples are inevitable for those doubly salient PM machines in which the PMs are located in the stator, hence offering much better mechanical integrity. Nevertheless, similar to other doubly salient PM machines, the torque ripples of these memory machines can readily be alleviated by optimizing the pole arcs of the salient poles in the stator and rotor, or applying the conduction angle control.

IV. Conclusion

In this paper, a new pole-changing approach has been proposed for the dual-memory machine. The key is to design the dual-memory machine with six PM poles in which four of them are based on 3-magnet PM poles (each PM pole is constituted by two Nd-Fe-B PM pieces and one Al-Ni-Co PM piece), and two of them are simple Al-Ni-Co PM poles. By reversely magnetizing the Al-Ni-Co PM pieces of the four 3-magnet PM poles, the Nd-Fe-B PM pieces are magnetically short-circuited, so-called the pole-dropping. The finite element analysis has validated this pole-changing approach. Compared with the single-memory machine, the dual-memory machine takes the advantages of higher power density, better stability, and easier pole-changing. However, it suffers from lower output torque when operating at the two-pole mode.

References

[1] K. T. Chau, C. C. Chan, and C. Liu, "Overview of permanent-magnet brushless drives for electric and ybrid electric vehicles," *IEEE Trans. Ind. Electron.*, vol. 55, no. 6, pp. 2246–2257, Jun. 2008.

[2] K. T. Chau and C. C. Chan, "Emerging energy-efficient technologies for hybrid electric vehicles," *Proc. IEEE*, vol. 95, no. 4, pp. 821–835, Apr. 2007.

[3] V. Ostovic, "Pole-changing permanent-magnet machines," *IEEE Trans. Ind. Appl.*, vol. 38, no. 6, pp. 1493–1499, Nov./Dec. 2002.

[4] K. Sakai and H. Hashimoto, "Permanent magnet motors to change poles and machine constants," in *Proc. Int. Conf. Elect. Mach.*, 2012, pp. 435–440.

[5] J. H. Lee and J. P. Hong, "Permanent magnet demagnetization characteristic analysis of a variable flux memory motor using coupled Preisach modeling and FEM," *IEEE Trans. Magn.*, vol. 44, no. 6, pp. 1550–1553, Jun. 2008.

[6] H. Liu, H. Lin, Z. Q. Zhu, M. Huang, and P. Jin, "Permanent magnet remagnetizing physics of a variable flux memory motor," *IEEE Trans. Magn.*, vol. 46, no. 6, pp. 1679–1682, Jun. 2010.

[7] C. Yu and K. T. Chau, "Design, analysis, control of DC-excited memory motors," *IEEE Trans. Energy Convers.*, vol. 26, no. 2, pp. 479–489, Jun. 2011.

[8] F. Li, K. T. Chau, C. Liu, and Z. Zhang, "Design principles of permanent magnet dual-memory machines," *IEEE Trans. Magn.*, vol. 48, no. 11, pp. 3234–3237, Nov. 2012.

[9] C. Yu and K. T. Chau, "Dual-mode operation of DC-excited memory motors under flux regulation," *IEEE Trans. Ind. Appl.*, vol. 47, no. 5, pp. 2031–2041, Sep./Oct. 2011.

[10] F. Li, K. T. Chau, C. Liu, J. Z. Jiang, and W. Y. Wang, "Design and analysis of magnet proportioning for dual-memory machines," *IEEE Trans. Appl. Supercond.*, vol. 22, no. 3, p. 4905404, Jun. 2012.